Article

Energy Monitoring and Analysis of a Residential House in China

Yanzhi Wang [1], Shaotong Han [2], Qiuqi Zhang [1], Jing Sun [1,3,*], Zhibao Cheng [1,3] and An Chen [1,3]

[1] School of Civil Engineering, Beijing Jiaotong University, Beijing 100044, China; 20115042@bjtu.edu.cn (Y.W.); 22125952@bjtu.edu.cn (Q.Z.); chengzb@bjtu.edu.cn (Z.C.); anchen@bjtu.edu.cn (A.C.)
[2] United World College Changshu China, Changshu 215556, China; sthan22@uwcchina.org
[3] Beijing's Key Laboratory of Structural Wind Engineering and Urban Wind Environment, Beijing Jiaotong University, Beijing 100044, China
* Correspondence: jsun@bjtu.edu.cn

Abstract: The energy consumption of residential buildings plays a crucial role in overall energy consumption and environmental sustainability. This paper aims to conduct an energy analysis of a residential house located in China, with a focus on comparing the accuracy of the model, identifying areas for improvement, and proposing energy-efficient solutions. Four sets of temperature sensors were placed to monitor the ambient temperature at which the building is located and the indoor temperature of the residential building during a heating season. The energy consumption of keeping the building running at a low temperature was recorded and compared with the simulation results to verify the accuracy of the model. The monitoring results give the weekly average temperature of each zone on each floor, and the door and window positions, room layouts, and orientations are discussed to analyze the thermal response of the building. In addition, the effect of the heat transfer coefficient of the exterior walls, the heat transfer coefficient of the roof, and the solar heat gain coefficient (SHGC) of the exterior windows on the heating energy consumption of the building are further analyzed through simulations. The results show that, after adding a certain thickness of insulation to the exterior walls and roofs of a building, increasing the thickness of the insulation layer produces little extra energy saving. The use of building windows with high SHGC can effectively reduce building heating energy consumption.

Keywords: residential building; energy monitoring; energy simulation; parametric study; optimization analysis

1. Introduction

With the progress and development of society, issues such as climate change and energy consumption have attracted widespread attention and discussion. Globally, the building sector constitutes approximately 36% of total energy consumption and over 40% of total carbon emissions. Among all sectors, the building industry possesses the greatest potential to implement effective energy saving measures [1,2]. In recent years, China has made significant efforts to address its energy consumption and environmental challenges. The residential sector, accounting for a substantial portion of the country's energy consumption, presents a unique opportunity for energy optimization [3]. As the country undergoes rapid urbanization and experiences a growing demand for housing, it becomes imperative to evaluate and analyze the energy performance of residential buildings. By analyzing the energy use of representative dwellings and proposing ideas for energy-optimized design, policymakers, architects, and owners can be guided to adopt more sustainable and energy-efficient building practices.

For the energy use of buildings, researchers' primary research methods include model simulation and field monitoring. Vartholomaio [4] used the dynamic building energy simulation software EnergyPlus 8.3 to perform a parametric simulation analysis of the heating and cooling energy consumption of residential buildings in three urban forms,

focusing on the Mediterranean city of Thessaloniki, which has a heating and cooling demand. The study concluded that there are synergies between a highly compact urban form and passive solar design. Additionally, Al-Saggaf et al. [5] integrated 3D building information modeling (BIM) models of three different design options for a residential building in Saudi Arabia using Ecotect analysis 2010 software for energy simulation. The results demonstrated the effectiveness of the Architectural-Based Energy Impact Scoring System (AEISS). Comprising seven building design features and over 40 design options, the AEISS exhibited a positive response. It effectively delivers energy-efficient and low-energy-consuming design options for decision-makers. Wang et al. [6] selected several typical buildings in Beijing as the research objects. They utilized eQUEST software to investigate the buildings' energy consumption and derived corresponding building energy consumption prediction model. These models can predict the overall energy consumption of various buildings types during urban regional planning stage, offering insights for urban energy conservation planning. Santana et al. [7] conducted a similar study, monitoring and comparing two dwellings in Barcelona, Spain, during the winter. Their analysis aimed to understand the impact of the envelope's thermal performance on indoor temperature, alongside other factors such as outdoor temperature and solar gain. This analysis suggested that a building's thermal performance involves multiple variables beyond envelope thermal transmittance, such as thermal inertia, solar gain building orientation, and an urban environment. Charai et al. [8] employed a validated PMV-PPD model in EnergyPlus to assess the benefits of using biosourced earth in building envelopes during the summer, based on real-time monitoring of an existing building. Results indicated that the proposed wall improved thermal comfort by regulating indoor temperature and humidity, with 24.6% fewer dissatisfied occupants compared to a typical wall. Shan et al. and Yu et al. [9,10] designed and constructed a test building to investigate the thermal performance of a new type of bamboo–steel composite wall. They measured the heat transfer coefficient of the composite wall and validated the simulation model through the actual measurement of the energy consumption of the test building. Simulation analyses were then carried out to investigate the energy saving effect of composite walls in different climatic regions. Hassan et al. [11] investigated the effects of courtyard layout, aspect ratio, and courtyard orientation on energy consumption in residential buildings using nine case studies. The results showed that the highest energy savings of 18.73% were achieved when the optimal location of the courtyard layout, i.e., southwest elevation, was adopted.

Further research on energy design optimization of buildings, based on building energy performance studies, can provide valuable insights for policymakers, architects, and building owners, fostering sustainable building development. In the realm of energy design optimization, many researchers have focused on reducing building energy consumption and enhanced indoor thermal comfort through modifications to the thermal performance of the building envelopes. Cabeza [12] conducted experiments on four small rooms constructed according to the traditional Mediterranean building system and compared the thermal performance of three typical insulation materials, polyurethane, polystyrene, and mineral wool, over an extended period. Tunçbilek et al. [13] indicated that the doping of highly conductive nanoparticles decreased the energy saving performance of phase change materials. The results showed that increasing the nanoparticle concentration to 3 vol% could increase the negative effect to 1.7%. Alyami et al. [14] investigated the effects of location and insulation materials on the energy performance of residential buildings across five climatic regions in the Kingdom of Saudi Arabia. Five commonly used insulation materials with distinct thermal properties, namely, polyurethane panels (PU), expanded polystyrene (EPS), glass wool (GW), urea–formaldehyde foam (UFF), and expanded perlite (EP), were analyzed in different climatic regions, revealing significant variations in energy performance of the insulation materials based on location. Guo et al. [15] constructed a comparative study between two identical model buildings, one insulated with 38 mm expanded polystyrene (EPS) panels as exterior insulation. The dynamic indoor thermal environment and heating energy consumption of both buildings were monitored compara-

tively at the same heating temperature. The results showed that the energy consumption of the two buildings was similar in the initial 20 min of heating, and the energy saving rate of the EPS building increased slowly with the heating duration. Amani et al. [16] modelled and analyzed the thermal behavior of buildings and identified design options to optimize building energy consumption and reduce global warming potential through an insulation system. The model incorporated a four-layer insulation system with the ability to select the material and thickness of each layer that offers 130 different design combinations. Other researchers have also proposed energy-efficient building designs focusing on cooling and heating loads and types of cooling and heating sources. Shibuya et al. [17] tested multistory office buildings at three different locations in Japan and investigated the potential impacts of climate change on the energy demand for office cooling and heating by simulating three periods of reference weather data through thermal analysis. The results emphasized the potential of office buildings in Japan for energy saving and CO_2 emissions reduction without relying on nuclear power generation. Li et al. [18] utilized DOE-2 software to simulate the cooling energy consumption and electricity demand in an office building in Hong Kong under various envelope performance and lighting systems, pointing out the importance of rational daylight use in the peak electricity consumption and peak cooling demand, and that appropriate lighting design could reduce the cooling energy consumption and electricity demand of buildings.

The aim of this paper Is to conduct energy monitoring and analysis of a residential building located in China, including the monitoring of outdoor/indoor temperatures and energy consumption of the building during a heating season, and analyze the thermal behavior of the building. The results from the energy analysis model are compared with the monitoring results to verify the validity of the model. On this basis, the heat transfer coefficients of the exterior wall and roof and the SHGC of the exterior window are taken as the key parameters to simulate and analyze the influence of the key parameters on the energy consumption of the building, providing a reference for the optimal design of the building's energy systems.

2. Building Information

2.1. Building Geometry

The demo house is a typical three-story reinforced concrete house in Haituo Valley, Zhangjiakou City, Hebei Province, China. Zhangjiakou is located at 39°30′–42°10′ N latitude and 113°50′–116°30′ E longitude, with a population of about 4.05 million in 2023, at an elevation of about 760 m above sea level, and has a temperate continental climate [19]. The photo of the building is shown in Figure 1. It is 7.7 m wide, 12.3 m long, and 9.9 m high. The main living room extends in height over all three floors. The total area of the demo house, including both heated and non-heated spaces, encompasses around 180 m^2. Of this, the heated area comprises approximately 144 m^2, providing comfortable living conditions during the colder months. The design and layout of the house were planned according to the codes in China, striking a balance between thermal comfort and energy consumption.

Figure 2 shows the location of the house and surrounding buildings, which are similar to the house in this study. Additionally, the house uses a shear wall structural system [20], which is also common. Furthermore, according to the *China Statistical Yearbook* [21], the per capita housing area in this region is 38.08 m^2. The house currently accommodates five people, resulting in a per capita housing area of approximately 36 m^2. Therefore, this house can be considered representative of the common housing typology in the region, and this study provides a reference for the energy consumption of the buildings in this region.

Overall, despite its elegance and functionality, the house's energy efficiency could be further improved. An analysis of its energy consumption can yield valuable insights into optimizing energy usage, enhancing sustainability, and promoting eco-friendly practices in residential construction. By identifying areas for improvement, such as insulation, the house can serve as a model for environmentally conscious residential design in the future.

Figure 1. Building photo.
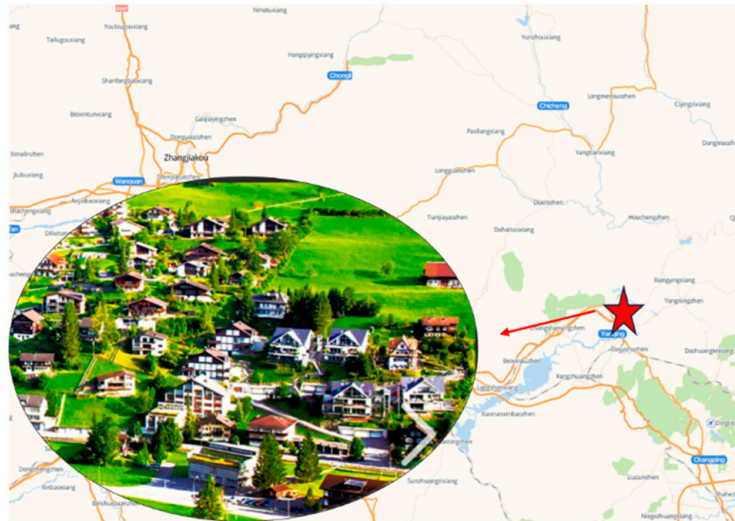
Figure 2. Geographical location of the house and surrounding buildings.

2.2. Building Construction

2.2.1. Wallboards

The exterior walls of the demo house are multi-layered, consisting of (from the exterior to the interior) a layer of 120 mm rock wool board, 10 mm cement mortar, 8 mm polymer mortar, and 200 mm reinforced concrete. The composite structure of the exterior wall and the interior wall are different. The interior walls that connect each room consist of a layer of 200 mm reinforced concrete and a 10 mm panel of cement mortar. The details of the structures are shown in Figure 3 and Table 1.
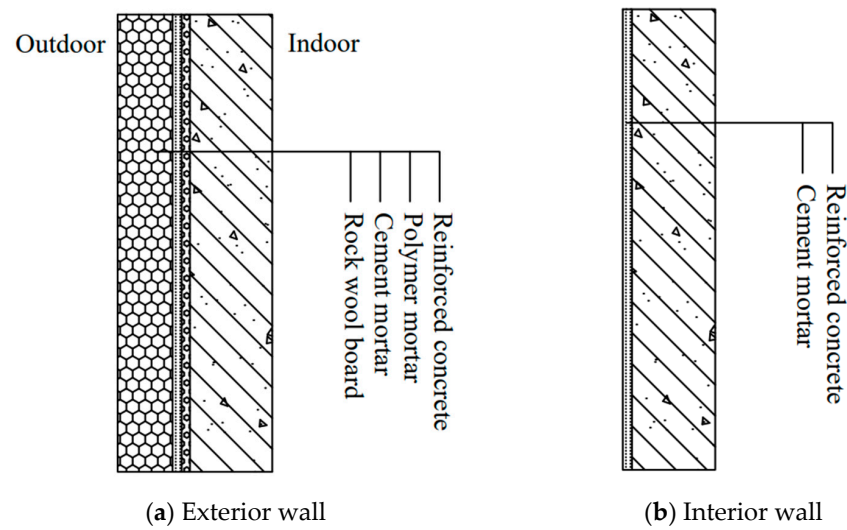
(**a**) Exterior wall   (**b**) Interior wall

Figure 3. Wallboard configuration.

Table 1. Building construction.

Building Component		Configuration	Thickness (mm)
Wallboards	Exterior wall	Reinforced concrete	200
		Polymer mortar	8
		Cement mortar	10
		Rock wool board	120
	Interior wall	Reinforced concrete	200
		Cement mortar	10
Roof		Fine stone concrete	40
		Plastic benzoic board	110
		SBS	4
		Cement mortar	15
		Reinforced concrete	150
Floor		Cement mortar	20
		Pisolite concrete	50
		Plastic benzoic board	20
		Cement mortar	20
		Reinforced concrete	120

2.2.2. Roof

The roof of the demo house consists of (from exterior to the interior) a layer of 40 mm fine stone concrete, 110 mm plastic benzoic board, 4 mm SBS (styrene–butadiene–styrene), 15 mm of cement mortar, and 150 mm reinforced concrete. The angle of the roof is 30° of elevation. The details are shown in Figure 4 and Table 1.
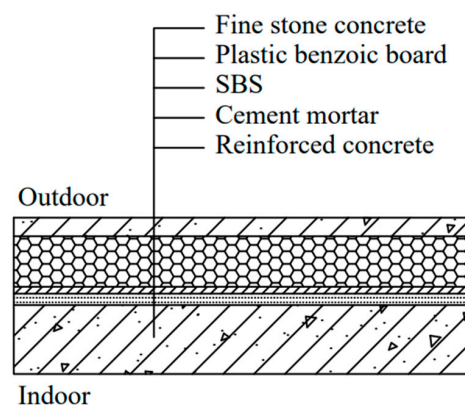

Figure 4. Roof configuration.

2.2.3. Floor

The floor of the demo house, in contact with the ground, is constructed of 120 mm reinforced concrete, 20 mm cement mortar, 20 mm plastic benzoic board, 50 mm pea gravel concrete, and 20 mm cement mortar. On the first floor and the second floor, they have the same structure as the floor that contacts with the ground. The details are shown in Figure 5 and Table 1.
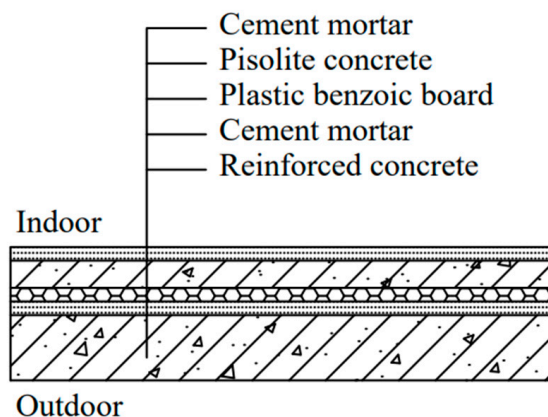

Figure 5. Floor configuration.

3. Methodology
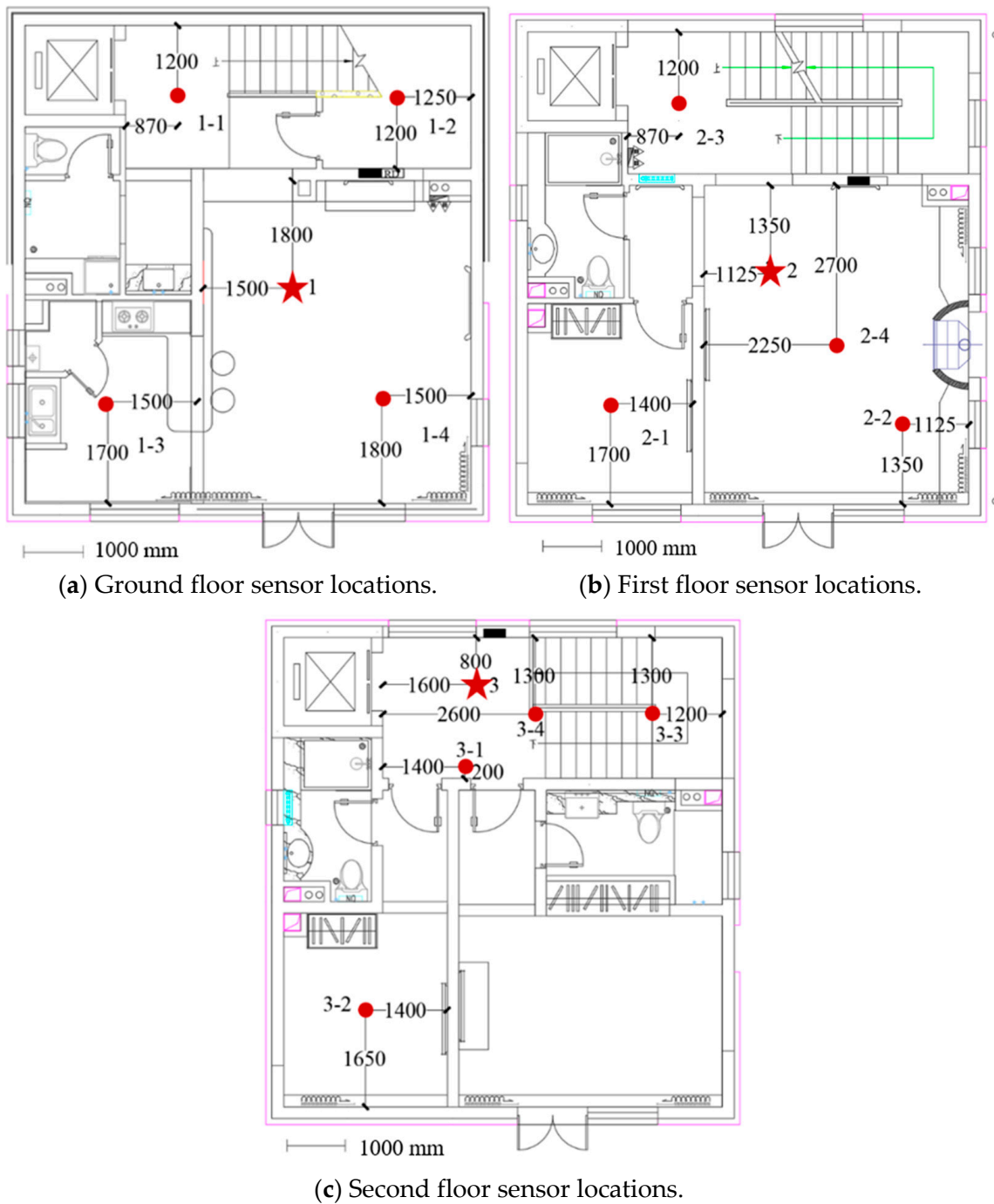
3.1. Monitoring Methodology

To analyze the thermal response of the building as well as to carry out 3D heat transfer model simulations, the average indoor temperatures of each zone on each floor of the building and the outdoor temperatures at the location of the building were monitored.

Temperature and humidity are important factors in building energy consumption. Studies have shown that buildings consume more energy in areas with higher humidity compared to those in dry environments [22–24]. The climate of this residence is temperate continental, which is relatively dry compared to areas such as the coast. Moreover, the building remains closed and unoccupied for most of the monitoring period, with only three days occupied. Therefore, humidity has a negligible effect on this building's energy consumption, and this study mainly focuses on temperature.

3.1.1. Indoor Average Temperature

A device for temperature monitoring of houses in low-temperature operations, the G9-TH instrument, was used, with data readings taken every 15 min. When selecting the sensor placement, several principles were followed: Firstly, representative rooms were chosen based on different orientations and floors. Secondly, the sensors were positioned to avoid interference from radiators and direct sunlight, ensuring a relatively stable temperature state. Additionally, the sensors were kept away from windows, considering that windows had higher heat transfer coefficients, which could result in localized temperature drops due to cold air infiltration. Furthermore, the sensors were placed at a horizontal distance of more than 0.5 m from the wall, with a recommended height between 0.6 m and 1.1 m.

On each floor, we installed four high-precision temperature sensors, and in addition, there was one main unit per floor, responsible for connecting and logging data from the four high-precision temperature sensors. The main unit was utilized to record the temperature measurements taken by the temperature sensors. The specific locations for sensor placement can be referred to in Figure 6, where the pentagram represents the main unit's position, and the circle denotes the position of the temperature sensor.

(**a**) Ground floor sensor locations.

(**b**) First floor sensor locations.

(**c**) Second floor sensor locations.

Figure 6. Locations of indoor temperature sensors (unit: mm): red color denotes sensors' locations, where the pentagram and circle indicate locations of the main unit and temperature sensor, respectively.

3.1.2. Outdoor Average Temperature

The sensors were placed in a well-ventilated area of the second-floor balcony to monitor the outdoor air temperature. Waterproofing was implemented to protect the sensors. The data recording interval was set to 15 min. The main unit 4 and 4-2 measurement points were positioned on the inner and outer sides of the living room's exterior wall, which were immediately adjacent to the windows, as shown in Figure 7. The pentagram and circle indicate the locations of the main unit and temperature sensor, respectively.
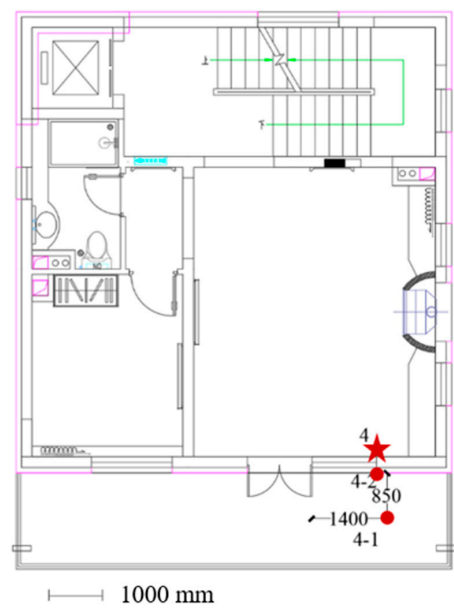
Figure 7. Locations of outdoor temperature sensors (unit: mm): red color denotes sensors' locations, where the pentagram and circle indicate locations of the main unit and temperature sensor, respectively.

3.1.3. Temperature Control

The house remained closed and unoccupied for the vast majority of the monitoring period, occupied for only a few days in mid-January. The indoor temperature of the building was controlled at 12 °C from November 1st to January 15th, 15 °C from January 16th to January 23rd, and 13 °C from January 24th to March 31st.

3.2. Modeling

We used SketchUp to model the house for accurate energy simulation in EnergyPlus, with the building model shown in Figure 8. The SketchUp model reflected the actual conditions of the base, which consisted of the three-story building located in Zhangjiakou. Due to significant temperature fluctuations between day and night in Zhangjiakou region, indoor temperatures were influenced by solar radiation during the daytime, resulting in substantial diurnal temperature variations. The temperature control settings in the model were consistent with the actual conditions. SketchUp enables zoning and supports zone-based modelling. In this study, different zones are divided, but the parameters are the same in each zone. Therefore, an in-depth discussion is not carried out.
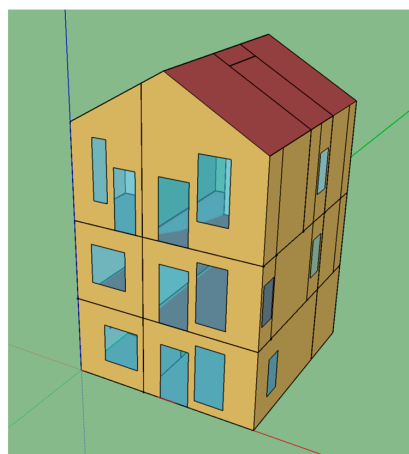
**Figure 8.** Building model (balconies not included).

The model used SketchUp, OpenStudio, and EnergyPlus, with a flowchart illustrated in Figure 9. First, SketchUp was used to construct the building's geometric model, which was then imported into OpenStudio, where building settings, including the building envelope, indoor thermal disturbances, etc., were configured. Subsequently, the OpenStudio model was exported as an IDF file, which was imported into EnergyPlus to complete the simulation process.
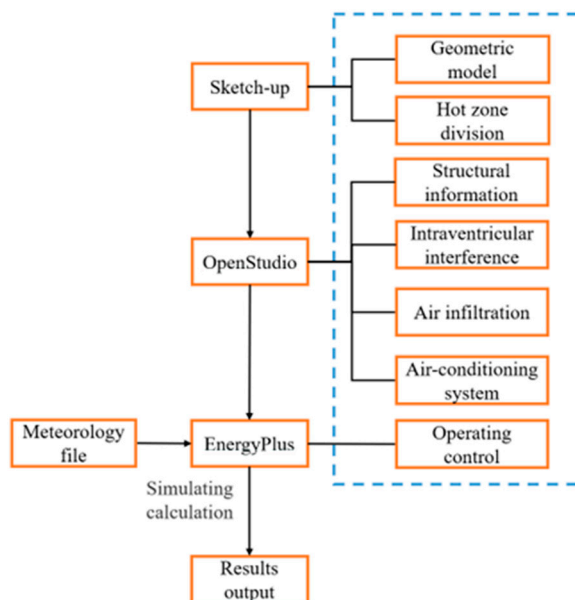
Figure 9. Modelling flowchart: blue dashed line represents settings and functions of each software.

Given that the sample building was a three-story structure in direct contact with the ground, the indoor temperatures were also affected by ground temperature. For our energy simulation in EnergyPlus, we incorporated temperature data that matched the actual conditions. To achieve this, we replaced the relevant portions of the typical meteorological year data from Huailai City with temperature data collected from outdoor temperature sensors placed around the sample building from December to April. The temperature data curve is shown in Figure 10. This replacement ensures a more accurate representation of local conditions in our temperature data.
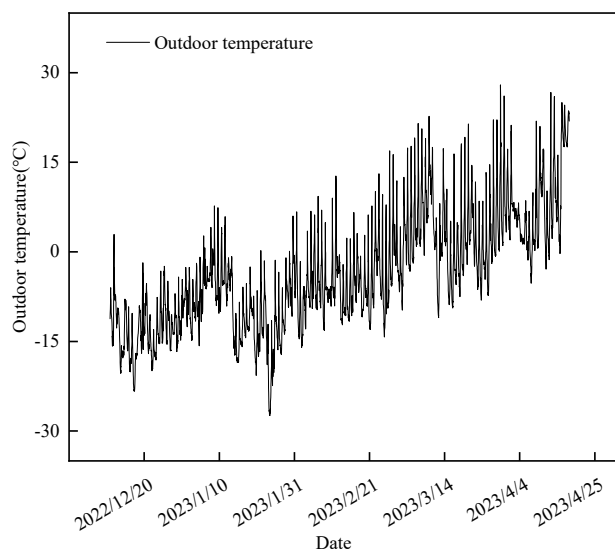
Figure 10. Outdoor temperature monitoring data.

Moreover, we set the average outdoor airflow velocity to match that around the sample building and included it in the EnergyPlus model. To further align the simulation with reality, we maintained consistency between the sample building and the model in terms of structural components, materials, thermal insulation coefficients, and heat transfer coefficients. The building remained closed and unoccupied for most of the monitoring period, with only three days occupied. The occupancy schedule for the three days and energy sources for different utilities are shown in Table 2. Since both lighting and domestic hot water were powered by electricity, it did not affect the gas consumption. Additionally, the building was occupied for only 3% of the monitoring period. Thus, the impact of occupancy and personnel, lighting, and electrical equipment on the building's energy consumption throughout the heating period was negligible. Therefore, thermal disturbance from personnel, lighting, and electrical appliances were not considered in this study. According to the Chinese standard JGJ/T 449-2018 [25], the space infiltration design flow rate, characterized by the indoor air change rate, was set as 0.5 times per hour, and the design specification outdoor air of the building was set as 0.008333 m^3/s per person. However, since this building was unoccupied during the monitoring period, there was no design specification outdoor air.

Table 2. Occupancy schedule and energy sources.

Time	House State	Energy Source		
		Lighting	**Domestic Hot Water**	**Heating**
2023/1/18–2023/1/20	Occupied	Electricity	Electricity	Gas
Other time	Vacant	-	-	Gas

During the modeling process, we segmented each room in the sample building to create distinct living zones. Our aim was to maximize the realism of the model and enable precise energy consumption simulations.

4. Results and Discussion

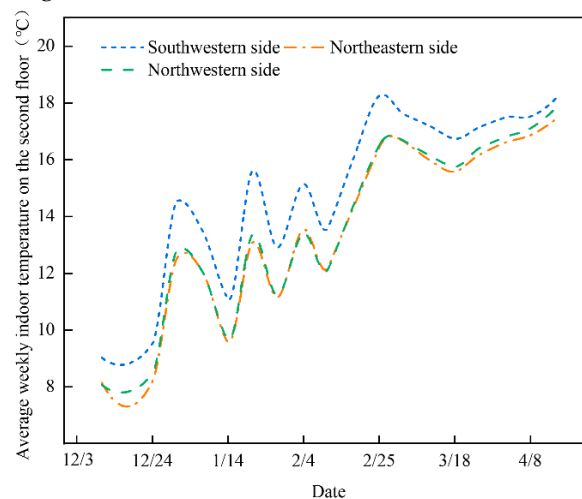### 4.1. Average Indoor Temperature Monitoring Results

The building was monitored for most of the period from December 2022 to mid-April 2023, with monitoring on the first floor interrupted from early March for maintenance reasons. During the monitoring period, the building remained closed and unoccupied for the vast majority of the time, with only a few days of occupancy, and the building kept the energy systems on to maintain low temperature operation. The following analysis focuses on the thermal response of the building systems.

Figure 11 shows the weekly average indoor temperatures for each zone on each floor of the building. Due to the lack of cooling equipment, the indoor temperatures often exceeded the control temperatures. All areas of the building were kept at low temperatures from December to February. From March onwards, due to the significant increase in outdoor temperatures, the indoor temperatures also increased significantly, often exceeding the control temperatures of the heating equipment. The monitoring results show that the temperature on the south side is higher than that on the north side, while the temperature on the southwestern side is significantly higher than that on the southeastern side, and the temperature on the northeastern side has small difference with that on the northwestern side. Such a pattern is reflected in all three floors of the building. The average indoor temperature on the southwestern side area of the ground floor is significantly higher than the other areas, while the average indoor temperature on the southeastern side of the ground floor is similar to that of the north side from December to February, and slightly higher than that of the north side after March. This can be attributed to the fact that the south side is exposed to more solar radiation than the north side, and that the rooms on the southwestern side of the ground floor are smaller than those on the southeastern side, resulting in less heat loss. In addition, the ground floor has a specialized structural form to provide better thermal insulation. It is on the outside of the rooms on the north side, which

may explain the smaller difference in average temperatures between the north and south sides of the ground floor compared with those of the first and second floors. The average indoor temperature on the southwestern side of the first floor is significantly higher than those of the other areas, while the average indoor temperature on the southeastern side is slightly higher than that on the north side, which is related to the orientation of the building, the layout of the rooms, and the location of the windows and doors. The rooms on the south side have large glass windows, which can receive more solar radiation, while the rooms on the southwestern side are much smaller than those on the southeastern side, and the heat loss is slower. The average indoor temperature on the southwestern side of the second floor is significantly higher than that on the north side, which is related to the fact that the south side receives more solar radiation. The temperature difference between the northwestern side and the northeastern side is not significant, which may be due to the location of the two areas and the common north-facing orientation.
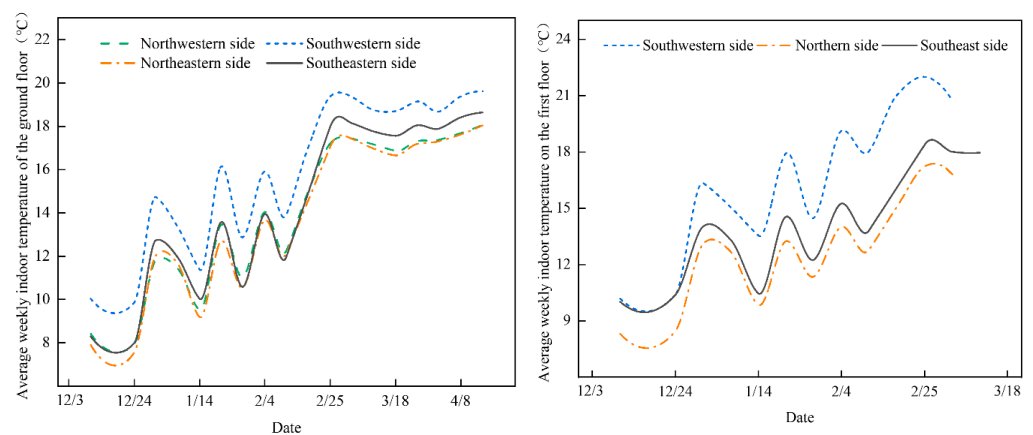
(**a**) Average weekly temperatures for each area of the ground floor.

(**b**) Average weekly temperatures for each area of the first floor.

(**c**) Average weekly temperatures for each area of the second floor.

Figure 11. Weekly average indoor temperatures for each zone on each floor of the building.

4.2. Building Heating Energy Consumption

During the monitoring period, we recorded outdoor and indoor temperatures and gas consumption. The actual energy consumption of building can be calculated based on the gas consumption. In the EnergyPlus model, the recorded outdoor and indoor temperatures were used as input values, based on which the building's energy consumption was calculated. In this case, it was considered that one cubic meter of natural gas produces

33,494.4 kJ of heat and the heating equipment used in the building, i.e., a gas wall oven, had a thermal efficiency of 85%.

The two results are shown in Table 3. After considering the thermal efficiency of the wall-hung gas boilers, the error between the simulated energy consumption and the actual energy consumption in each month is around 10%, which indicates that the 3D heat transfer model built with EnergyPlus can effectively simulate the energy consumption of the building. The monitoring began from December 10. Therefore, the actual outdoor temperature of the building in November and some days in December was missing. During the simulation, the outdoor temperature of the building was based on the weather data in the typical meteorological year file offered by EnergyPlus, resulting in lower simulation accuracy in November and December. In March, the error was at 17.68%, which was larger than the other months because the property only recorded the actual gas consumption of the building for one week.

Table 3. Monthly comparison of simulated and actual energy consumption.

	November	December	January and February	March
Simulate building heating energy consumption (GJ)	3.00	9.80	17.55	0.75
Simulate building gas consumption (m^3)	105.37	344.22	616.43	26.34
Actual building gas consumption (m^3)	124	396	657	32
Percentage (%)	84.98	86.92	94.37	82.32
NMBE (%)		-12.57		
CV(RMSE) (%)		12.18		
R^2 (%)		90		

To calibrate the accuracy of the model, three metrics were employed, i.e., NMBE, CV (RMSE) [26], and linear regression (R^2), based on monthly energy consumption. Since only one week's data were recorded in March, this month was excluded from the calculation. The results are shown in Table 3, where NMBE, CV (RMSE), and R^2 are -12.57%, 12.18%, and 90%, respectively. It can be seen that NMBE and CV (NMBE) are within the tolerance of ±20% specified by the International Performance Measurement and Verification Protocol (IPMVP) [26] and 15% specified by American Society of Heating, Refrigerating and Air-Conditioning Engineers (ASHRAE) Guideline 14-2014 [27], respectively. In addition, R^2 is much higher than the criteria of 75% [28]. Therefore, the 3D model developed above can be considered accurate and will be used in the following parametric analysis. A similar model was also calibrated in a previous work [29].

4.3. Parametric Analysis

4.3.1. Parameter Selection

About 50% of the building energy loss is through the envelope. Therefore, improving the thermal performance of the building envelope is an effective way to save energy in buildings [30–32]. The year-round dynamic energy simulation of the building model was carried out by EnergyPlus software, and the heat transfer coefficients of the envelope exterior walls and roofs as well as the solar heat gain coefficients of the exterior windows were taken as the key parameters [33–36]. The parameters of the original scheme of the building were used as benchmarks for adjusting each of the key parameters and analyzing the influence of each key parameter on the energy efficiency of the building, as shown in Table 4.

The heat transfer coefficient of the exterior wall of the original program of the building was 0.3114 W/(m^2·K). The increase in the heat transfer coefficient of the exterior wall was achieved by increasing the thickness of the exterior wall insulation material. Adding a layer of rock wool board for the exterior wall in the model, the thickness changed from 10 mm to 300 mm, the thermal resistance increased in the range of 0.2439~7.317 m^2·K/W,

and the corresponding heat transfer coefficient of the exterior wall changed in the range of 0.2894~0.0950 W/(m^2·K).

Table 4. The simulated parameters, variables, and variations of the variables.

	Insulating Layer Thickness (mm)	Thermal Resistance (m^2·K/W)	Heat Transfer Coefficient (W/(m^2·K))
Exterior wall	10~300	0.2439~7.317	0.2894~0.0950
Roof	10~300	0.2439~7.317	0.2277~0.0887

The roof heat transfer coefficient for the original building was 0.2523 W/(m^2·K). The increase in roof heat transfer coefficient was achieved by increasing the thickness of the roof insulation. By adding a layer of rock wool board for the roof in the model, the thickness changed from 10 mm to 300 mm, the thermal resistance increased in the range of 0.2439 to 7.317 m^2·K/W, and the corresponding roof heat transfer coefficient changed in the range of 0.2277 to 0.0887 W/(m^2·K).

The SHGC of the building's original program for the exterior windows was 0.4. The effect of the SHGC on the building's energy consumption is seasonal, with smaller SHGC yielding lower energy consumption in the summer months and larger SHGC yielding lower energy consumption in the winter months. Since the monitoring of the building as well as the modeling in this paper focuses on the winter heating energy consumption of the building, higher parameter values than the original scheme were chosen, with a parameter variation range of 0.42 to 0.6.
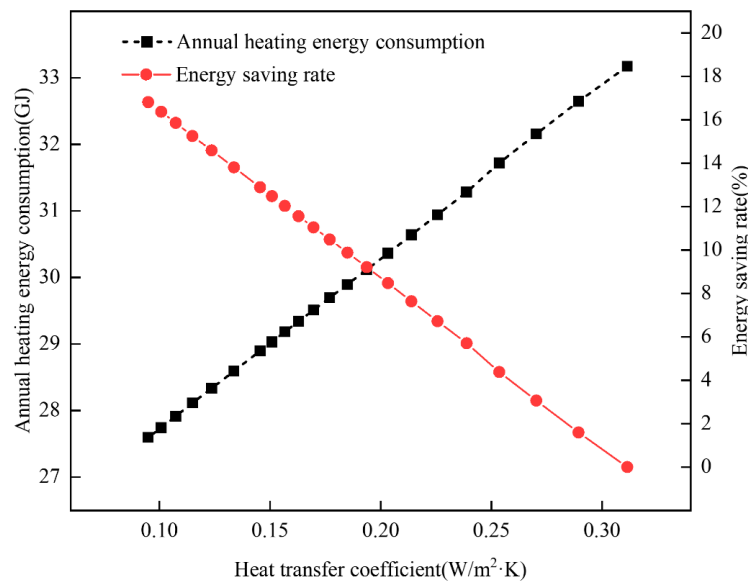
4.3.2. Analysis of Simulation Results

(1) Influence of Heat Transfer Coefficients of Exterior Walls on Building Heating Energy Consumption

Energy Plus software was used to carry out energy consumption simulation based on the above parameters, and only the heat transfer coefficient of the exterior wall was changed, while other parameters were kept unchanged to carry out energy consumption simulation for the whole year. Changing the heat transfer coefficient of the exterior wall was achieved by increasing the thermal resistance value of the exterior wall. The effect of increasing the thermal resistance of the exterior wall on the energy consumption of the building heating is shown in Figure 12, and the relationship between the heat transfer coefficient of the exterior wall, which corresponds to increasing the thermal resistance of the exterior wall, and the energy consumption of the building's heating is shown in Figure 13.

The annual heating energy consumption of the building decreases gradually as the thermal resistance of the exterior wall increases from 0.2439 m^2·K/W to 7.317 m^2·K/W, and the corresponding heat transfer coefficient of the exterior wall decreases from 0.2894 W/(m^2·K) to 0.0950 W/(m^2·K). The annual heating energy consumption of the building and the heat transfer coefficient of the exterior wall are basically linearly related, and the annual heating energy consumption decreases linearly with the reduction in heat transfer coefficient of the exterior wall. The energy saving rate is also linearly related to the heat transfer coefficient of the exterior wall, and the energy saving rate increases linearly with the decrease in heat transfer coefficient of the exterior wall. From the point of view of increasing the thermal resistance of the exterior wall, increasing the thermal resistance causes the annual heating energy consumption of the building to gradually decrease, but the decreasing trend gradually becomes slower. The energy saving rate increases with increasing thermal resistance, but the increasing trend also slows down significantly. For example, when a 130 mm thick rock wool board is added to the exterior wall of the building as an insulation layer, the energy saving rate increases by less than 0.5% compared to a 120 mm thick insulation layer. The simulation results show that after adding a certain thickness of insulation layer to the exterior wall of the building, increasing the thickness of the insulation layer does not result in a satisfactory energy saving effect.
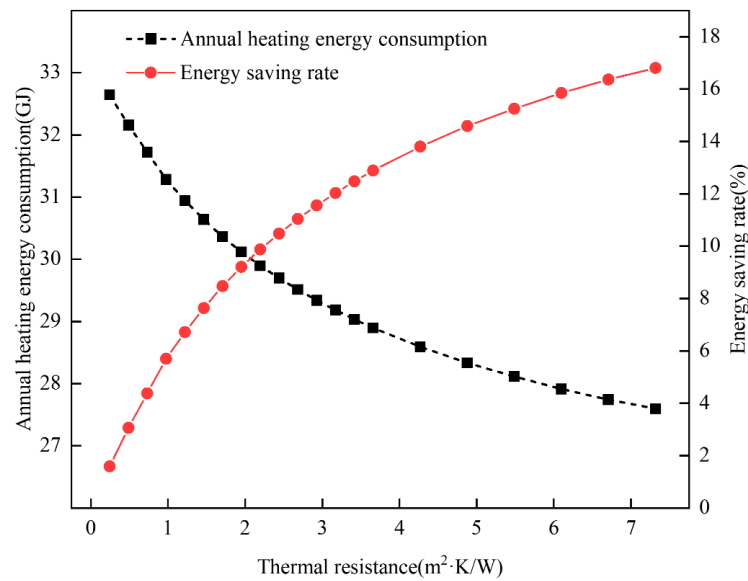
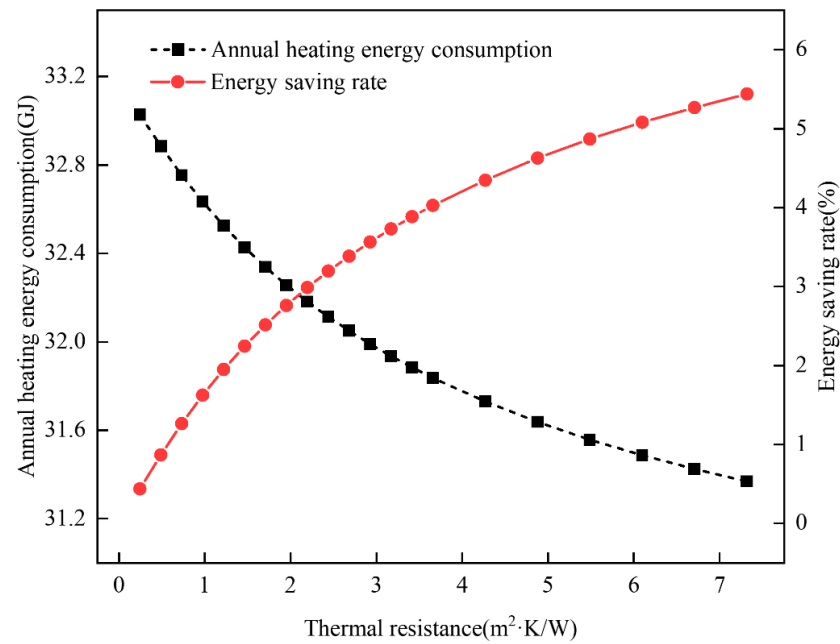**Figure 12.** Influence of the thermal resistance of exterior walls on building heating energy consumption.

Figure 13. Influence of heat transfer coefficients of exterior walls on building heating energy consumption.

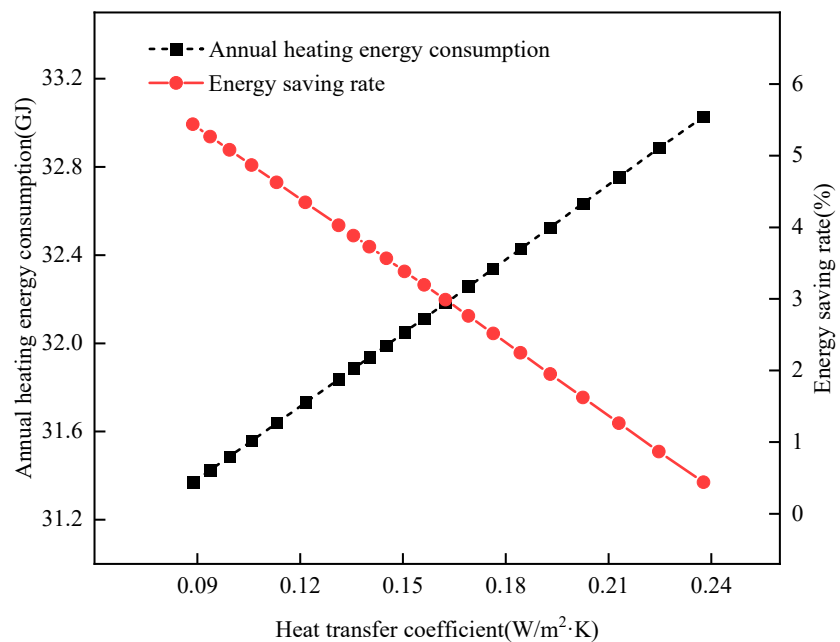(2) Influence of Roof Heat Transfer Coefficient on Building Heating Energy Consumption

In this section, only the roof heat transfer coefficient was changed, and the values of the building's original scheme for the other parameters were adopted. Changing the heat transfer coefficient of the roof was achieved by increasing the thermal resistance value of the roof. The effect of increasing the thermal resistance of the roof on the building heating energy consumption is shown in Figure 14, and the relationship between the heat transfer coefficient of the roof—which corresponds to increasing the thermal resistance of the roof—and the building heating energy consumption is shown in Figure 15.

The annual heating energy consumption of the building decreases gradually as the value of the roof thermal resistance increases from 0.2439 m²·K/W to 7.317 m²·K/W, and the corresponding heat transfer coefficient of the exterior wall decreases from 0.2277 W/(m²·K) to 0.0887 W/(m²·K). The annual heating energy consumption of the building is linearly related to the roof heat transfer coefficient, and the annual heating energy consumption decreases linearly with the decrease in roof heat transfer coefficient. The energy saving rate is also linearly related to the roof heat transfer coefficient, and the energy saving rate

increases linearly with the decrease in roof heat transfer coefficient. From the point of view of increasing the thermal resistance of the roof, increasing the thermal resistance causes the annual heating energy consumption of the building to decrease gradually, but the decreasing trend gradually becomes slower. The energy saving rate increases with the increase in thermal resistance, but the increasing trend also gradually becomes slower. When 110 mm thick rock wool boards are added to the roof of the building as an insulation layer, the energy saving rate increases by less than 0.2% compared to a 100 mm thick insulation layer. The simulation results show that, after adding a 100 mm thick layer of insulation to the building roof, further increase in the thickness of the insulation produces little extra energy saving.


Figure 14. Influence of roof thermal resistance on building heating energy consumption.

Figure 15. Influence of roof heat transfer coefficient on building heating energy consumption.

(3) Influence of Exterior Window Solar Heat Gain Coefficient on Building Heating Energy Consumption

In this section, only the solar heat gain coefficient of the exterior windows was changed, and the values of other parameters were adopted from the original scheme of the building to simulate the energy consumption for the whole year. The effect of increasing the solar heat gain coefficient of the exterior windows on the heating energy consumption of the building is shown in Figure 16.
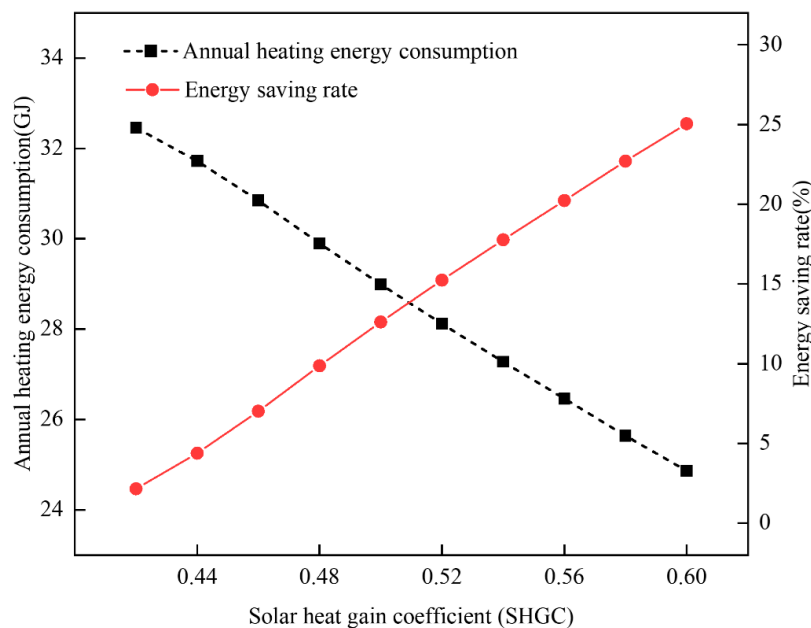
Figure 16. Influence of exterior window solar heat gain coefficients on building heating energy consumption.

As the solar heat gain coefficient of the exterior window increases from 0.42 to 0.6, the amount of indoor heat gain from solar radiation through the window gradually increases, and the annual heating energy consumption of the building decreases linearly. With the increase of each 0.02 in the solar heat gain coefficient of the exterior window, the annual heating energy consumption of the building decreases by 0.7143, 0.7407, 0.8726, 0.9451, 0.9107, 0.8727, 0.8395, 0.8150, 0.8217, and 0.7780 GJ, respectively, and the annual heating energy consumption of the building and the solar heat gain coefficient of the exterior window basically shows a linear relationship. The energy saving rate also increases linearly with the increase in solar heat gain coefficient of exterior windows. For every 0.02 increase in the solar heat gain coefficient of exterior windows, the energy saving rate increases by 2.23%, 2.63%, 2.85%, 2.75%, 2.63%, 2.53%, 2.46%, 2.48%, and 2.35%, respectively, and the energy saving rate is basically linearly related to the solar heat gain coefficient of exterior windows. The simulation results show that the use of building exterior windows with higher solar heat gain coefficients can effectively reduce building heating energy consumption.

5. Conclusions

This paper reports the energy monitoring and analysis of a typical residential house situated in the Haituo Valley of northern Beijing, a region with sub-zero temperatures in winter and mild temperatures in summer. Based on this study, the following conclusions can be drawn:

1. The monitoring results showed that the indoor temperature on the south side of the building was higher than that on the north side, while the temperature on the southwest side was significantly higher than that on the southeast side, and the temperature difference between the northwest and northeast sides was small. This is

related to the orientation of the building, the layout of the rooms, the position of the doors and windows, and the special structure of the ground floor.

2. A 3D model of the building was constructed using EnergyPlus, and the building structural information, room temperature control, and other parameters were consistent with the actual situation. Comparing simulation results with actual energy consumption data, the error between the two values is around 10%, proving the accuracy of the EnergyPlus model.

3. The results from the EnergyPlus model are more accurate when the outdoor temperature is based on the monitoring data, compared with those when the outdoor temperature is based on the typical meteorological year file.

4. The EnergyPlus model was further employed to analyze the impact of enhancing the thermal resistance of the exterior envelope on the building's energy efficiency. The results show that, after adding a certain thickness of thermal insulation to the building's wall and roof, the energy saving effect produced by further increasing the thickness of the thermal insulation layer is limited.

5. By analyzing the influence of exterior window solar heat gain coefficient on the building's energy efficiency, it can be concluded that the use of building exterior windows with a higher solar heat gain coefficient can effectively reduce building energy consumption.

This study illustrates the effectiveness of using EnergyPlus in assessing building energy performance and highlights the significance of window design in energy conservation efforts. These findings offer valuable insights for optimizing building designs and promoting energy-efficient practices in construction.

6. Limitations and Future Work

According to the energy monitoring and analysis of the residential house in China, the following suggestions and recommendations for future research are made:

1. Residential energy is a significant source of global growth in energy demand and carbon emissions. The location characteristics, housing characteristics, and unit size of a home all affect the energy use of residential buildings, which still needs to be explored.

2. Some parameters, such as external window heat transfer coefficient, window-to-wall ratio, and humidity, also impact building energy consumption, but are not included in this study, which can be considered in future research.

3. The specified air exchange value, which refers to the rate at which indoor air is replaced by outdoor air, is directly related to the thermal environment and energy consumption of a building. Appropriate air exchange rate helps maintain indoor air quality and provides a comfortable living and working environment. An excessively high air exchange rate can lead to significant energy loss through the ventilation system, thereby increasing the building's energy consumption. Therefore, it is worth studying the impact of different air exchange rates on the energy consumption of buildings in future research.

Author Contributions: Conceptualization, J.S., Z.C. and A.C.; Data curation, S.H. and Q.Z.; formal analysis, Y.W. and Q.Z.; funding acquisition, J.S. and A.C.; investigation, Y.W. and Q.Z.; methodology, Y.W. and Q.Z.; project administration, J.S. and A.C.; resources, J.S. and A.C.; software, Y.W., S.H. and Q.Z.; supervision, J.S., Z.C. and A.C.; validation, Y.W., S.H. and Q.Z.; writing—original draft, Y.W., S.H. and Q.Z.; writing—review & editing, J.S., Z.C. and A.C. All authors have read and agreed to the published version of the manuscript.

Data Availability Statement: The data presented in this study are available on request to the corresponding author.

Conflicts of Interest: The authors declare no conflict of interest.

References

1. International Energy Agency. *Energy Efficiency: Buildings. The Global Exchange for Energy Efficiency Policies, Data and Analysis*; International Energy Agency: Paris, France, 2022.
2. Du, X.; Wen, L.; Wei, P.; Yang, M. A systematic approach for analyzing building energy conservation and emission reduction policies based on the principle of WSR. *Energy Build.* **2024**, *315*, 114328. [CrossRef]
3. Cai, W. *China Building Energy Consumption Annual Report 2020*; China Association of Building Energy Efficiency: Xiamen, China, 2020.
4. Vartholomaios, A. A parametric sensitivity analysis of the influence of urban form on domestic energy consumption for heating and cooling in a Mediterranean city. *Sustain. Cities Soc.* **2017**, *28*, 135–145. [CrossRef]
5. Al-Saggaf, A.; Nasir, H.; Taha, M. Quantitative approach for evaluating the building design features impact on cooling energy consumption in hot climates. *Energy Build.* **2020**, *211*, 109802. [CrossRef]
6. Wang, R. *Simulation and Prediction of Typical Building Energy Consumption in Beijing*; Xi'an University of Architecture and Technology: Xi'an, China, 2018.
7. Santana, B.O.; Torres-Quezada, J.; Coch, H.; Isalgue, A. Monitoring and Calculation Study in Mediterranean Residential Spaces: Thermal Performance Comparison for the Winter Season. *Buildings.* **2022**, *12*, 325. [CrossRef]
8. Charai, M.; Mezrhab, A.; Moga, L. A structural wall incorporating biosourced earth for summer thermal comfort improvement: Hygrothermal characterization and building simulation using calibrated PMV-PPD Model. *Build. Environ.* **2022**, *212*, 108842. [CrossRef]
9. Shan, Q.; Tong, K.; Zhang, X.; Li, Y. Field Test and Simulation Analysis of Thermal Performance of Bamboo Steel Composite Wall in Different Climate Regions. *Adv. Civ. Eng.* **2020**, *2020*, 1–10. [CrossRef]
10. Yu, D.; Tan, H.; Ruan, Y. A future bamboo-structure residential building prototype in China: Life cycle assessment of energy use and carbon emission. *Energy Build.* **2011**, *43*, 2638–2646. [CrossRef]
11. Seddik Hassan, A.M.; Abd El Aal, R.F.A.; Fahmi, A.A.E.; Ali, S.M.A.; Abdelhady, M.I. Courtyard geometry's effect on energy consumption of AlKharga city residential buildings, Egypt. *Sci. Rep.* **2024**, *14*, 11149. [CrossRef]
12. Cabeza, L.F.; Castell, A.; Medrano, M.; Martorell, I.; Pérez, G.; Fernández, I. Experimental study on the performance of insulation materials in Mediterranean construction. *Energy Build.* **2010**, *42*, 630–636. [CrossRef]
13. Tunçbilek, E.; Arıcı, M.; Krajčík, M.; Li, Y.; Jurčević, M.; Nižetić, S. Impact of nano-enhanced phase change material on thermal performance of building envelope and energy consumption. *Int. J. Energy Res.* **2022**, *46*, 19313–20900. [CrossRef]
14. Alyami, S.H.; Alqahtany, A.; Ashraf, N.; Osman, A.; Aldossary, N.A.; Almutlaqa, A.; Al-Maziad, F.; Alshammari, M.S.; Al-Gehlani, W.A.G. Impact of Location and Insulation Material on Energy Performance of Residential Buildings as per Saudi Building Code (SBC) 601/602 in Saudi Arabia. *Materials.* **2022**, *15*, 9079. [CrossRef] [PubMed]
15. Guo, L.; Liao, Y.; Cheng, Z.; Zheng, H.; Guo, L.; Long, E. Experimental study on dynamic effect of exterior insulation on indoor thermal environment and energy consumption. *Energy Build.* **2022**, *274*, 112299. [CrossRef]
16. Amani, N.; Kiaee, E. Developing a two-criteria framework to rank thermal insulation materials in nearly zero energy buildings using multi-objective optimization approach. *J. Clean. Prod.* **2020**, *276*, 122592. [CrossRef]
17. Shibuya, T.; Croxford, B. The effect of climate change on office building energy consumption in Japan. *Energy Build.* **2016**, *117*, 149–159. [CrossRef]
18. Li, D.H.W.; Lam, J.C.; Wong, S.L. Daylighting and its effects on peak load determination. *Energy.* **2005**, *30*, 1817–1831. [CrossRef]
19. Dong, H.R.; Liu, J.P. Analysis of Thermal Performance and Energy Consumption of Residential Envelope Structures in Zhangjiakou City. *Heat. Vent. Air Cond.* **2003**, *33*, 3.
20. Han, J.; Lu, X.; Gu, Y.; Liao, W.; Cai, Q.; Xue, H. Optimized data representation and understanding method for the intelligent design of shear wall structures. *Eng. Struct.* **2024**, *315*, 118500. [CrossRef]
21. National Bureau of Statistics of China. *China Statistical Yearbook*; China Statistics Press: Beijing, China, 2020.
22. Sowa, J.; Mijakowski, M. Humidity-Sensitive, Demand-Controlled Ventilation Applied to Multiunit Residential Building—Performance and Energy Consumption in Dfb Continental Climate. *Energies* **2020**, *13*, 6669. [CrossRef]
23. Lou, R.; Hallinan, K.P.; Huang, K.; Reissman, T. Smart Wifi Thermostat-Enabled Thermal Comfort Control in Residences. *Sustainability.* **2020**, *12*, 1919. [CrossRef]
24. Wang, Y.; Liu, K.; Liu, Y.; Wang, D.; Liu, J. The impact of temperature and relative humidity dependent thermal conductivity of insulation materials on heat transfer through the building envelope. *J. Build. Eng.* **2022**, *46*, 103700. [CrossRef]
25. *JGJ/T 449-2018*; Standard for green performance calculation of civil buildings. China building industry press: Beijing, China, 2018.
26. Efficiency Valuation Organization. *International Performance Measurement & Verification Protocol: Concepts and Options for Determining Energy and Water Savings*; Technical Report; Efficiency Valuation Organization: Washington, DC, USA, 2012.
27. American Society of Heating, Refrigerating, and Air-Conditioning Engineers. *ASHRAE Guideline 14-2014: Measurement of Energy, Demand, and Water Savings*; Technical Report; American Society of Heating; Refrigerating, and Air-Conditioning Engineers: Atlanta, GA, USA, 2014.
28. Pachano, J.E.; Bandera, C.F. Multi-step building energy model calibration process based on measured data. *Energy Build.* **2021**, *252*, 111380. [CrossRef]

29. Sun, J.; Zhang, Q.; Chen, A.; Wu, Z. Energy performance of buildings with multi-ribbed composite wall structural system. *J. Build. Eng.* **2024**, *91*, 109614. [CrossRef]
30. Manz, H.; Frank, T. Thermal simulation of buildings with double-skin façades. *Energy Build.* **2005**, *37*, 1114–1121. [CrossRef]
31. Omrany, H.; Ghaffarianhoseini, A.; Ghaffarianhoseini, A.; Raahemifar, K.; Tookey, J. Application of passive wall systems for improving the energy efficiency in buildings: A comprehensive review. Renew. *Sustain. Energy Rev.* **2016**, *62*, 1252–1269. [CrossRef]
32. Ginevičius, R.; Podvezko, V.; Raslanas, S. Evaluating the alternative solutions of wall insulation by multicriteria methods/Pastatų sienų šiltinimo variantų vertinimas taikant daugiakriterius metodus. *J. Civ. Eng. Manag.* **2008**, *14*, 217–226. [CrossRef]
33. Zhu, J.; Chew, D.A.; Lv, S.; Wu, W. Optimization method for building envelope design to minimize carbon emissions of building operational energy consumption using orthogonal experimental design (OED). *Habitat Int.* **2013**, *37*, 148–154. [CrossRef]
34. Maučec, D.; Premrov, M.; Leskovar, V.Ž. Use of sensitivity analysis for a determination of dominant design parameters affecting energy efficiency of timber buildings in different climates. *Energy Sustain. Dev.* **2021**, *63*, 86–102.
35. Liao, W. *Research on Energy Saving of Building Envelope Structure in Nanjing Area Based on DeST Simulation*; Anhui University of Science and Technology: Huainan, China, 2018.
36. Li, H. *Research on Energy Simulation and Energy Saving of an Office Building in Hot Summer and Cold Winter Area*; Harbin Institute of Technology: Harbin, China, 2020.